In Situ Structure Evolution from Cu(OH)$_2$ Nanobelts to Copper Nanowires

Zhong Lin Wang* and Xiang Yang Kong

Schools of Materials Science and Engineering, Georgia Institute of Technology, Atlanta, Georgia 30332-0245

Xiaogang Wen and Shihe Yang

Department of Chemistry, Institute of Nano Science and Technology, The Hong Kong University of Science and Technology, Clear Water Bay, Kowloon, Hong Kong

In situ structural evolution from Cu(OH)$_2$ nanobelts to copper nanowires has been studied by transmission electron microscopy in a vacuum of 3×10^{-8} Torr. The decomposition follows the sequence of Cu(OH)$_2 \rightarrow$ CuO $\rightarrow$ Cu$_2$O $\rightarrow$ Cu. The decomposition from Cu(OH)$_2$ to CuO is attributed to electron beam radiation damage. The reduction from CuO to Cu$_2$O is attributed to heat-induced decomposition between 50 and 200 °C. For the Cu(OH)$_2$ nanobelts synthesized using the copper grid with and without a carbon coating, the decomposition from Cu$_2$O to Cu takes place between 200 and 300 °C and 300 and 600 °C, and the final Cu takes the forms of polycrystalline nanowires sheathed with graphitic carbon and nanoparticles, respectively. Therefore, because of the nanostructured nature of the nanowires and large surface area, introducing carbon into the sample synthesis can reduce the decomposition temperature by almost half. This study demonstrates a possible approach for creating metallic copper nanowires by heat-induced decomposition under vacuum at 300 °C or even lower.

Introduction

Since the discovery of oxide nanobelts,[1,2] the synthesis of beltlike quasi-one-dimensional nanostructures has attracted a great deal of attention. Nanobelts of ZnO,[1] SnO$_2$,[1] In$_2$O$_3$,[1] CdO,[1] Ga$_2$O$_3$,[3] PbO,[4] ZnS,[5] MgO,[6] and GaN[7] have been synthesized by a solid−vapor phase process. The as-synthesized oxide nanobelts are pure, structurally uniform, and single-crystalline, and most of them are free of dislocations. The nanobelts have a rectangular-like cross section, and their surfaces are well-defined crystallographic planes. The beltlike morphology appears to be a unique and common structural characteristic of the family of semiconducting oxides with cations of different valence states and materials of distinct crystallographic structures. Using the geometry and properties offered by the nanobelts, field-effect transistors[8] and gas sensors[9] have been fabricated by using single nanobelts. Nanoresonators[10] and nanocantilevers[11] have also been demonstrated using nanobelts.

Copper-based nanowires and nanobelts are of great interest because of their application as interconnects for microelectronics. Copper nanowires and related structures have been synthesized by physical and chemical techniques. The reduction of CuCl$_2$ at 300 °C results in the formation of Cu nanowires.[12] Copper rods have been grown by in situ heating a copper grid in a transmission electron microscope to 815 °C in a vacuum of 1.0×10^{-6} Torr.[13] Cu$_2$S nanowires have been synthesized by reacting Cu with H$_2$S[14] and have been used as template for the synthesis of Cu(OH)$_2$ nanoribbons through a solution-phase approach.[15] CuO nanowires have been fabricated by oxidizing metallic copper in the atmosphere at 400−600 °C.[16,17] It maybe easier to create oxide nanostructures by oxidizing metals, but the reverse process of creating metal nanowires using oxides

as templates may not be easy. In this paper, we report a detailed study of the decomposition process from Cu(OH)$_2$ nanobelts to metallic copper nanowires by in situ transmission electron microscopy. The structural evolution occurs in a few steps (Cu(OH)$_2 \rightarrow$ CuO $\rightarrow$ Cu$_2$O $\rightarrow$ Cu), but the temperature required for each step is different. We will also demonstrate the critical role played by carbon in reducing the decomposition temperature.

Material Synthesis. The Cu(OH)$_2$ nanobelts were synthesized using Cu$_2$S nanowires as the precursor materials. First, copper grids used for transmission electron microscopy were used as metal substrates for the fabrication of Cu$_2$S nanowires in the atmosphere of O$_2$/H$_2$S = 1.0 and with a reaction time of 10 h.[15] Second, Cu$_2$S nanowires were used as the copper source for the synthesis of Cu(OH)$_2$ nanobelts under basic conditions.[15] Before further reactions for the preparation of Cu(OH)$_2$ nanobelts, the Cu$_2$S nanowires on the copper grids were washed with an aqueous solution of HCl (1.0 M) for ∼20 min and subsequently with deionized water three times to remove surface impurities. The Cu$_2$S nanowires on the copper grids were then immersed into an aqueous solution of ammonia (Aldrich, 0.01 M, pH = 9−10). After reacting for 2 h, a blue layer was formed on the surface of the substrates. Finally, the samples were taken out of the reactor after a given reaction time, washed with deionized water three times, and dried in air. Two types of copper grids were used: one with a carbon film coating and the other without carbon, which will be shown to have a drastic effect on the reducing temperature.

X-ray diffraction (XRD) analysis was performed on a Philips PW 1830 X-ray diffractometer with a 1.5405-Å Cu Kα rotating anode point source. Transmission electron microscopy (TEM) observations were conducted at 200 kV using a Hitachi HF-2000 FEG TEM. A heating stage for the Hitachi HF-2000 FEG TEM was used for in situ experiments. The precision of

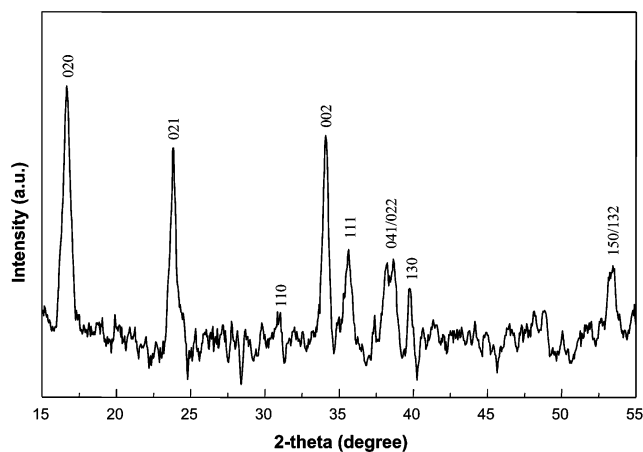* To whom correspondence should be addressed. E-mail: zhong.wang@mse.gatech.edu.

Figure 1. X-ray spectrum of the synthesized $Cu(OH)_2$ nanobelts.

measuring the local temperature with a thermocouple is ± 15 °C. A typical in situ TEM observation took about 4 h to raise the temperature from room temperature to 600 °C, during which time the images and diffraction data were recorded. The average heating rate was ~2−5 °C/min.

Results and Discussions

Structure of the As-Synthesized Samples. The structure of the as-synthesized specimen was first examined by X-ray diffraction. The XRD pattern shown in Figure 1 is attributable to the orthorhombic $Cu(OH)_2$ phase with lattice parameters of $a = 0.29463$, $b = 1.05437$, and $c = 0.52377$ nm, which are in good agreement with the corresponding literature values: $a = 0.29471$, $b = 1.05930$, and $c = 0.52564$ nm.[18] The chemical composition of the as-synthesized nanoribbon was determined previously by X-ray photoelectron spectrum (XPS) and the Cu Auger electron spectrum.

The TEM image clearly shows the nanobelt shape of the as-synthesized $Cu(OH)_2$ (Figure 2a). Each nanobelt is composed of tiny nanostructured grains that were created during the reaction in solution but has a uniform geometrical shape as defined by the template of Cu_2S. The size distribution of the nanobelts is very narrow. The ribbon shape can be directly seen through the twist of the nanobelts. The electron diffraction pattern recorded from the region agrees with the proposed $Cu(OH)_2$ structure (Figure 2b), which is indexed on the basis of the orthorhombic crystal structure of space group *Cmcm* (63).

In-Situ Decomposition Process. The in-situ TEM observation was carried out in a vacuum of 3×10^{-8} Torr inside a TEM. The TEM image and corresponding electron diffraction pattern were recorded from the same region of the sample as a function of the local temperature. To track the structural evolution and transformation from $Cu(OH)_2$ to Cu, electron diffraction patterns representing different phases are investigated in detail. For the purpose of building up the standards, four electron diffraction patterns corresponding to the phases of $Cu(OH)_2$, CuO, Cu_2O, and Cu are compared and indexed in Figure 3. These diffraction patterns were acquired at some typical temperatures as indicated during the experiments. The indexes are given on the basis of the following structural information. The $Cu(OH)_2$ phase has an orthorhombic structure with space group *Cmcm* (63) and lattice parameters $a = 0.295$, $b = 1.059$, and $c = 0.527$ nm. CuO has a monoclinic structure with space group *C2/c* (15) and lattice parameters $a = 0.468$, $b = 0.342$, $c = 0.513$, and $\beta = 99.55°$. Cu_2O has a cubic structure with space group *Pn3m* (224) and lattice constant $a = 0.427$ nm. Copper has cubic structure with space group
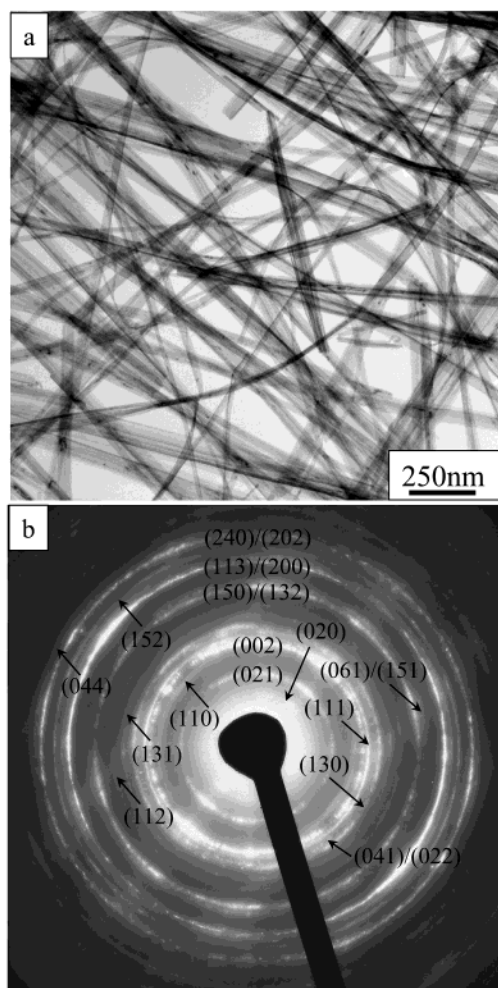

Figure 2. Bright-field TEM image of $Cu(OH)_2$ nanobelts (a) and the corresponding select-area electron diffraction pattern (b).

Fm3m (225) and lattice constant $a = 0.3615$ nm. These patterns will be used to trace the structural evolution process during the in situ decomposition process.

Specimen 1: Reduction with the Presence of Carbon. Two types of samples have been examined. The first type of samples is the $Cu(OH)_2$ nanobelts prepared using copper grids coated with carbon during the solution reaction. Figure 4 shows a series of TEM images and the corresponding electron diffraction patterns recorded at some typical temperatures at which some visible structure transformations occurred. The phases are determined by comparing the observed patterns to the typical patterns displayed in Figure 3. The as-synthesized sample at 25 °C was $Cu(OH)_2$ (Figure 4a), but soon after raising the temperature to 35 °C, it transformed into CuO although there was no visible change in the image, indicating the high instability of $Cu(OH)_2$ in vacuum and under the electron beam. It is thought that the radiation introduced by the electron beam expedited the decomposition process especially for $Cu(OH)_2$, but the electron dosage was kept low to minimize the damage. For the decomposition of other phases, the effect from the electron beam, especially for a Hitachi HF-2000 TEM with a cold field-emission source, is fairly low and spread. As the temperature was raised higher than 55 °C, a fraction of the nanobelts started to transform into Cu_2O (Figure 4c); this process continued to 150 °C and even beyond (Figure 4d), and again there was no visible change in the morphology of the nanobelts. The decomposition from CuO to Cu_2O was nearly complete
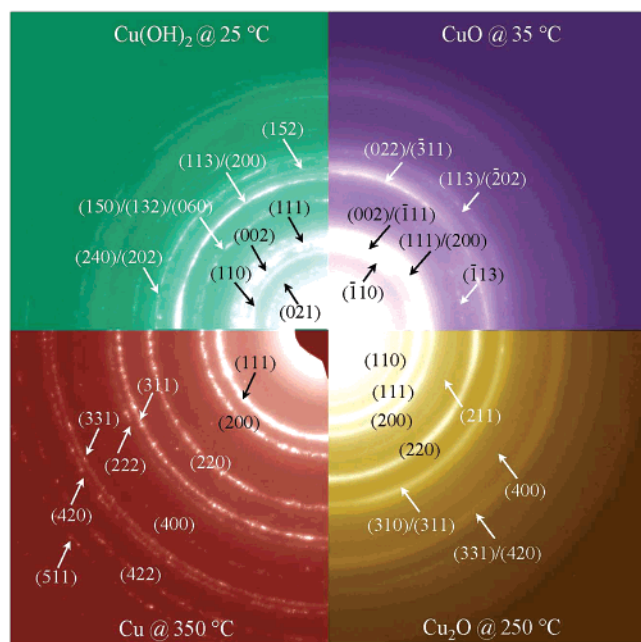
Letters

J. Phys. Chem. B, Vol. 107, No. 33, 2003 **8277**

Figure 3. Select-area electron diffraction patterns corresponding to nanostructures of $Cu(OH)_2$, CuO, Cu_2O, and Cu. The patterns were selected from the in situ experiments, which will be used to identify the structural evolution process during in situ experiments.

when the temperature reached 250 °C (Figure 4e), at which point some tiny particles with visible contrast appeared in the image. Some copper particles were formed when the temperature reached 300 °C (Figure 4f). By keeping the specimen at 300 °C for 12 h[21] in the TEM without turning on the electron beam, a complete reduction from Cu_2O to Cu occurred (Figure 4g); some crystalline copper nanowires were formed. Further increases in temperature resulted in no more phase transformations (Figure 4h). It is the temperature that induces the decomposition from Cu_2O to Cu at 300 °C.

The phase transformation is dominated not only by temperature but also by kinetics. The structural evolution as displayed in Figure 4 occurs over a range of temperature, and the amount of the reduced compound depends on the length of time at a particular temperature. It is observed by the bright-field TEM image in Figure 4e that small Cu particles were formed at 250 °C. A comparison between the bright-field image and a corresponding dark-field TEM image shows the presence of Cu particles of sizes 5−10 nm (Figure 5). The distribution of the Cu particles is uniform.

The nanowires formed by the in-situ heating process were examined by high-resolution TEM. The overall morphology of the copper nanowires is fairly uniform, and their diameters range from 20 to 80 nm (Figure 6a). The nanowires are polycrystalline; some Cu particles can also be identified (Figure 6b). The Cu nanowires are sheathed by a thin layer of carbon (Figure 6c and d), which may come from the carbon coated on the copper grid used for synthesizing the $Cu(OH)_2$ nanobelts. By removing the Cu nanowire core, carbon nanotubes may be recovered.[19] A high-resolution TEM image recorded near the interface between carbon and Cu clearly shows the 0.34-nm graphitic fringes, and the Cu {111} fringes of 0.21 nm are also present (Figure 6e). The role played by carbon in the structural evolution process will be discussed next.

Specimen 2: Decomposition without Carbon. The second type of sample used for our study was $Cu(OH)_2$ grown on copper grids without a carbon coating. Starting from the as-synthesized $Cu(OH)_2$ (Figure 7a), the transformation to CuO was complete

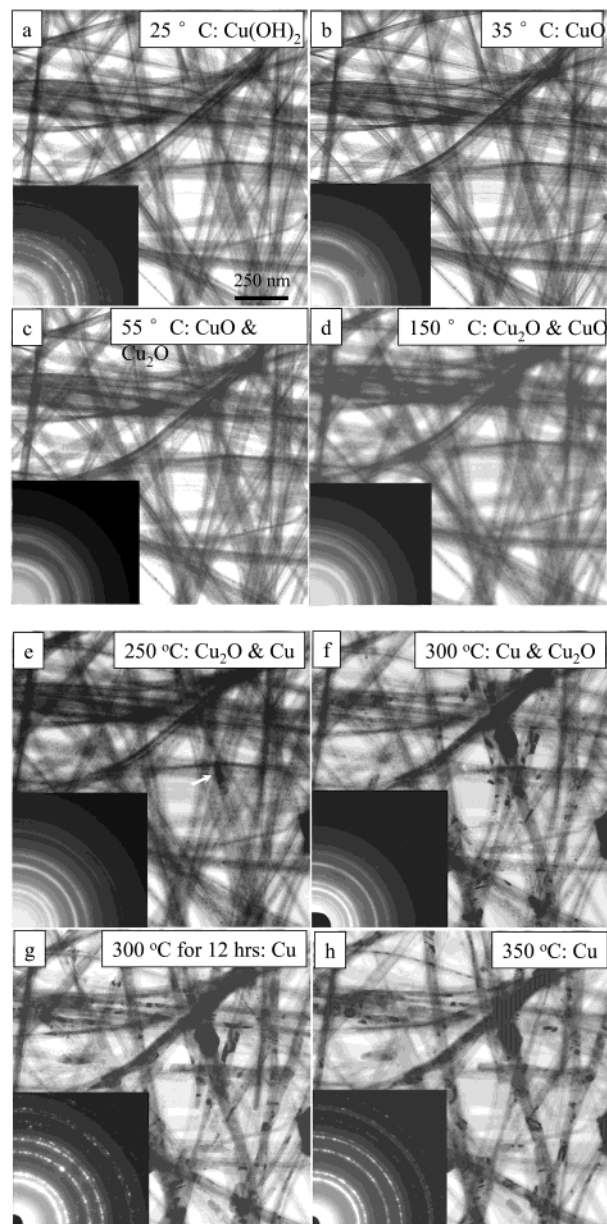**Figure 4.** Series of in situ TEM images and corresponding select-area electron diffraction patterns taken from a $Cu(OH)_2$ sample that was grown from a copper TEM grid coated with a carbon film while being heated to different temperatures.

at temperatures as low as 50 °C (Figure 7b). From 50−250 °C, the decomposition from CuO to Cu_2O was completed (Figure 7c). There is no major change in the image although there are some tiny particles appearing in the nanobelt. From 250 to 300 °C, Cu_2O was quite stable even after the sample was kept at 300 °C for over 12 h in the TEM, showing the stability of Cu_2O under these conditions.

Some small Cu particles started to form at temperatures above 300 °C (Figure 8a), and the particles grew larger after keeping the sample at 305 °C for 12 h in the TEM (particles A−D) (Figure 8b). The size of the particles remained unchanged after raising the temperature to 400 °C (Figure 8c), and even to 520 °C (Figure 8d), the corresponding electron diffraction patterns prove that the phases were a mixture of Cu_2O and Cu although the content of Cu_2O decreased as the temperature rose. The reduction from Cu_2O to Cu was almost finished when the temperature reached 600 °C (Figure 8e and f). The sizes of particles A−D remain unchanged from 520 to 600 °C.
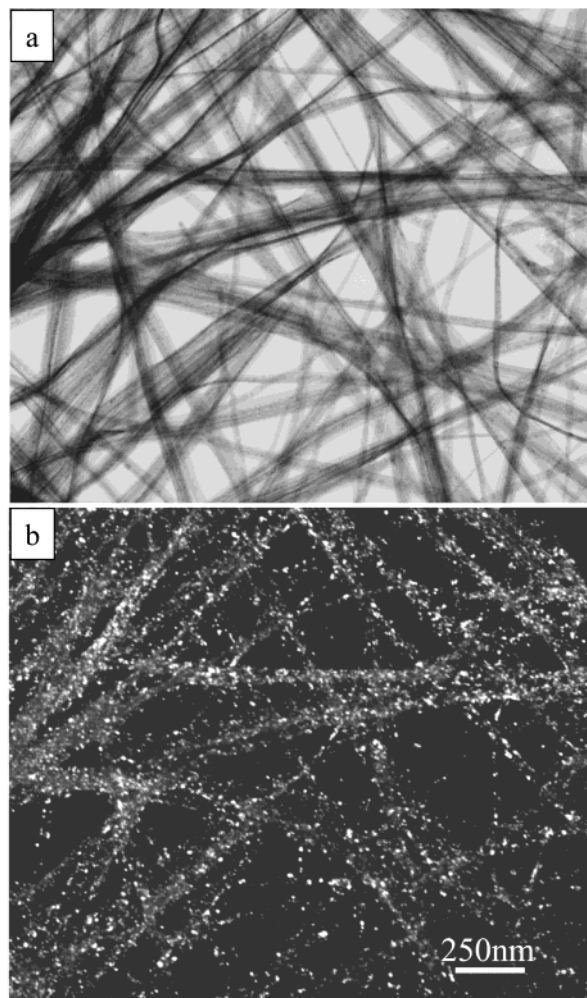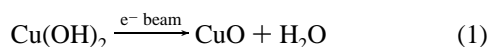
Figure 5. Bright-field TEM image of Cu(OH)₂ after heating at 250 °C overnight (a) and corresponding dark-field TEM image (b) where the small Cu particles display a bright contrast.
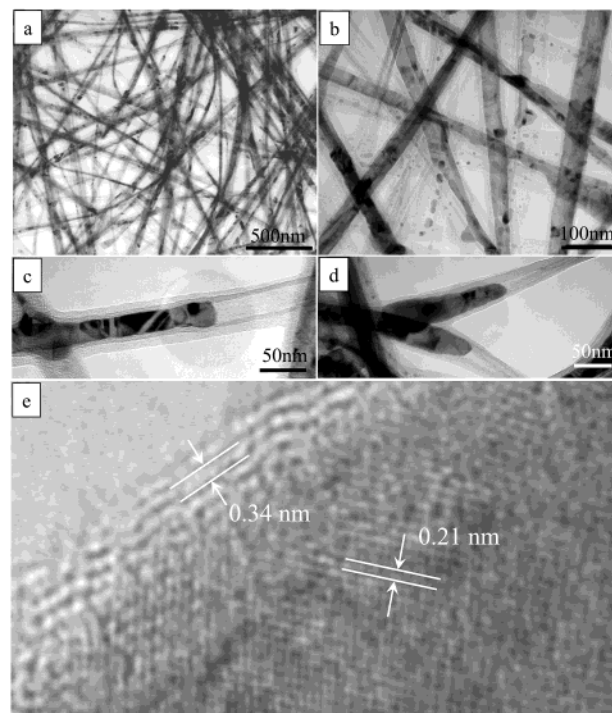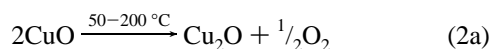

Figure 6. (a, b) Typical low-magnification TEM images of Cu nanowires. (c, d) Copper wires/rods sheathed by a graphitic layer, showing a cable structure. (e) HRTEM image of a Cu nanowire.
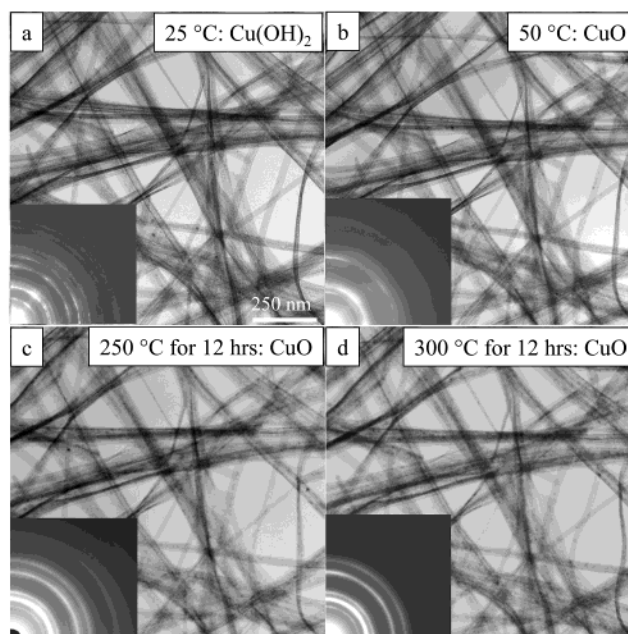
A high-resolution TEM analysis of the Cu nanowires is presented in Figure 9. The nanowires are polycrystalline, and there is no specific orientational relationship among the grains. The Morie fringes created by the double diffraction between two grains along the electron beam are visible at the bottom right corner. A Fourier transform of the circled region in the image clearly proves its face-centered-cubic structure.

Discussion

By comparing the results received from the samples prepared with and without the presence of carbon during the synthesis, we can make two points. First, the decomposition from Cu(OH)₂ to CuO occurs almost instantly under the electron beam and in vacuum, suggesting that this process is likely due to electron beam radiation damage rather than heating, which could be stated as

$$Cu(OH)_2 \xrightarrow{\text{e}^- \text{ beam}} CuO + H_2O \qquad (1)$$

The other point is that the decomposition from CuO to Cu₂O is at about the same temperature range of 50−200 °C and is likely due to thermally induced decomposition:

$$2CuO \xrightarrow{50-200\ ^{\circ}C} Cu_2O + {}^1/_2 O_2 \qquad (2a)$$

Figure 7. Series of in situ TEM images and corresponding select-area electron diffraction patterns taken from a Cu(OH)₂ sample that was grown from a copper TEM grid without a carbon coating while being heated to different temperatures.

The lower temperature required for this decomposition is likely due to the high vacuum and large surface areas for small crystals. For the sample with the presence of carbon, the following process is also possible:

$$2CuO + C \xrightarrow{50-200\ ^{\circ}C} Cu_2O + CO \qquad (2b)$$

The coating of carbon on the as-synthesized nanostructure is likely to occur during the growth of the nanobelts. Ex situ
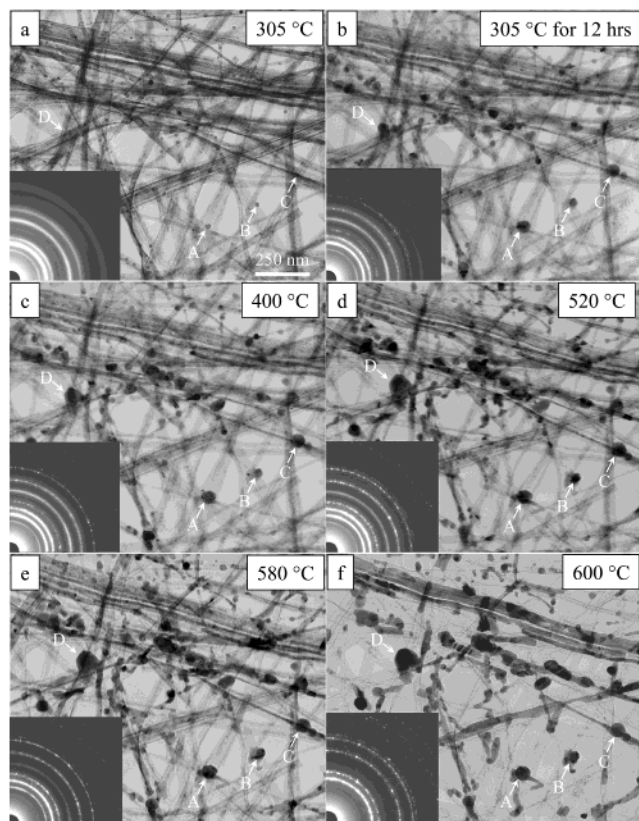
Letters

J. Phys. Chem. B, Vol. 107, No. 33, 2003 **8279**

Figure 8. Series of in situ TEM images and corresponding select-area electron diffraction patterns taken from a Cu(OH)$_2$ sample that was grown from a copper TEM grid without a carbon coating while being heated to different temperatures.
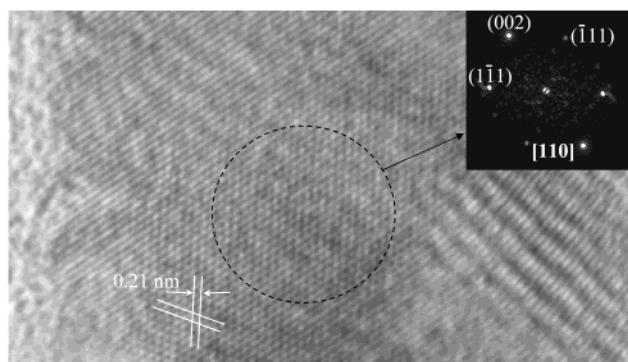

Figure 9. HRTEM image of a Cu nanowire. The inset is the corresponding Fourier transform of the image in the circled region.

decomposition from CuO to Cu$_2$O has been carried out by Kaito et al.,[16] who found that the decomposition took place at 300–400 °C. The lower temperature found in our experiments is probably due to a better vacuum.

Two major differences are observed. The temperature range required for the reduction from Cu$_2$O to Cu is quite different for the samples with and without carbon. The temperature for the sample with carbon is 200–300 °C, and it is 300–600 °C for the sample without carbon. The morphology of the reduced Cu is also quite distinctive. The striking difference between Figure 8f and Figure 4g is that the final product is dominated by Cu nanowires for the sample with carbon and Cu particles are formed for the sample without the presence of carbon. The results support the fact that carbon can assist the reduction

process and that it can reduce the reduction temperatures, which are

$$Cu_2O + C \xrightarrow{200-300 \,°C} Cu + CO \qquad (3)$$

and

$$Cu_2O \xrightarrow{300-600 \,°C} 2Cu + {}^1\!/_2O_2 \qquad (4)$$
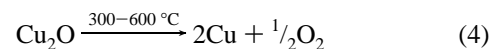
The relatively lower temperature in reaction 3 led to the formation of copper nanowires as defined by the templates of original Cu(OH)$_2$. The reduction process (eq 4) is a heat-induced decomposition. The melting point of nanoparticles is about $^1\!/_3$ to $^1\!/_2$ of the bulk melting temperature, depending on the particle size[20] (the melting point of Cu bulk is 1083 °C), thus 400–600 °C is high enough to melt the nanoparticles, at least at the surface; hence higher temperature results in the formation of Cu nanoparticles instead of nanowires for the sample without the presence of carbon.

Conclusions

In situ structural evolution from Cu(OH)$_2$ nanobelts to copper nanowires has been observed by transmission electron microscopy in a vacuum of 3×10^{-8} Torr. The decomposition follows the sequence Cu(OH)$_2 \rightarrow$ CuO $\rightarrow$ Cu$_2$O $\rightarrow$ Cu. The decomposition from Cu(OH)$_2$ to CuO occurs within a short period of time under a 200-kV electron beam, which is attributed to radiation damage. The decomposition from CuO to Cu$_2$O takes place within a temperature range of 50–200 °C, which is attributed to the heat-induced decomposition. For the Cu(OH)$_2$ nanobelts synthesized using the copper grids with a carbon coating, the reduction from Cu$_2$O to Cu takes place between 200 and 300 °C, and the final Cu takes the form of nanowires sheathed with graphitic carbon. The nanowires are made of polycrystalline copper grains, and the carbon prevents the copper from oxidizing. For the Cu(OH)$_2$ nanobelts synthesized using the copper grid without a carbon coating, the reduction from Cu$_2$O to Cu occurs between 300 and 600 °C, and the final Cu nanostructure takes the form of nanoparticles because of the melting induced by the higher annealing temperature. Therefore, introducing carbon into the synthesis can reduce the reduction temperature to almost *half* in the final reduction from oxide Cu$_2$O to metallic Cu. It must be pointed out that the temperature required to induce the reduction or decomposition also depends on the nanostructured nature and surface area of the sample. The small grain size can rapidly expedite the rate of oxygen diffusion. This study demonstrates a possible technique for creating metallic copper nanowires by heat-induced reduction under vacuum at 300 °C or even lower. This result may have applications in semiconductor processing and microsystem integration based on copper technology.

References and Notes

(1) Pan, Z. W.; Dai, Z. R.; Wang, Z. L. *Science* **2001**, *291*, 1947.
(2) Dai, Z. R.; Pan, Z. W.; Wang, Z. L. *Adv. Funct. Mater.* **2003**, *13*, 9.
(3) Dai, Z. R.; Pan, Z. W.; Wang, Z. L. *J. Phys. Chem. B* **2002**, *106*, 902.
(4) Pan, Z. W.; Dai, Z. R.; Wang, Z. L. *Appl. Phys. Lett.* **2001**, *80*, 309.
(5) Ma, C.; Moore, D.; Li, J.; Wang, Z. L. *Adv. Mater.* **2003**, *15*, 228.
(6) Ma, R. Z.; Bando, Y. *Chem. Phys. Lett.* **2003**, *370*, 770.

(7) Jian, J.; Chen, X. L.; He, M.; Wang, W. J.; Zhang, X. N.; Shen, F. *Chem. Phys. Lett.* **2003**, *368*, 416.

(8) Arnold, M.; Avouris, P.; Pan, Z. W.; Wang, Z. L. *J. Phys. Chem. B* **2002**, *107*, 659.

(9) Comini, E.; Faglia, G.; Sberveglieri, G.; Pan, Z. W.; Wang, Z. L. *Appl. Phys. Lett.* **2002**, *81*, 1869.

(10) Bai, X. D.; Gao, P. X.; Wang, Z. L.; Wang, E. G. *Appl. Phys. Lett.* **2003**, *82*, 4806.

(11) Hughes, W. L.; Wang, Z. L. *Appl. Phys. Lett.* **2003**, *82*, 2886.

(12) Yemn, M. Y.; Chiu, C. W.; Hsia, C. H.; Chen, F. R.;, Kai, J. K.; Lee, C. Y.; Chiu, H. T. *Adv. Mater.* **2003**, *15*, 235.

(13) Liu, Z.; Bando, Y. *Adv. Mater.* **2003**, *15*, 303.

(14) Wang, S.; Yang, S. *Chem. Mater.* **2001**, *13*, 4794.

(15) Wen, X.; Zhang, W.; Yang, S. H.; Dai, Z. R.; Wang, Z. L. *Nano Lett.* **2002**, *2*, 1397.

(16) Kaito, C.; Nakata, Y.; Saito, Y.; Naiki, T.; Fujita, K. *J. Cryst. Growth* **1986**, *74*, 469−479.

(17) Jiang, H.; Herricks, T.; Xia, Y. *Nano Lett.* **2002**, *2*, 1333.

(18) Oswald, H. R.; Reller, A.; Schmalle, H. W.; Dubler, E. *Acta Crystallogr.*, *Sect. C* **1990**, *46*, 2279.

(19) Suzuki, H.; Fukuzawa, N.; Tanigaki, T.; Sato, T.; Kido, O.; Kimura, Y.; Kaito, C. *J. Cryst. Growth* **2002**, *244*, 168.

(20) Buffat, Ph.; Borel, J. P. *Phys. Rev. A* **1976**, *13*, 2287.

(21) Hereafter, the 12-h experiment was carried out overnight by turning off the electron beam, but the vacuum was maintained and the temperature was applied.